CREEP RESPONSE OF AUSTENITIC STAINLESS STEEL FOILS FOR ADVANCED RECUPERATOR APPLICATIONS

Hassan Osman and Mohd Nasir Tamin
Faculty of Mechanical Engineering, Universiti Teknologi Malaysia
81310 UTM Skudai, Johor, Malaysia

ABSTRACT The severe operating conditions of elevated temperature and high pressure of a recuperator foil elements accelerate creep deformation and moisture-induced material degradation. This study is aimed at extending the operating temperature limit of AISI 347 austenitic stainless steel foils in view of maintaining cost competitiveness of the recuperator materials. In this respect, a series of constant load creep-rupture tests are performed on AISI 347 steel foils of thickness 0.25 mm at 700 °C and different load levels. The as-processed (rolled and annealed) foils displayed austenite matrix with transformed carbide precipitates. Results show that the creep life of AISI 347 steel foil samples is dominated by the secondary and tertiary creep stages. The steady-state creep region is characterized by the power-law creep. Phase analysis of creep-ruptured samples indicates the presence of $Cr_{23}C_6$ and NbC along the grain boundaries. Creep cavitations at triple-point grain boundaries are also observed.

1. INTRODUCTION

The development of clean and efficient microturbine system (100 kWe) utilizing natural gas is being proposed. Such microturbine employs compact, high efficiency heat-exchanger or recuperator. A typical thin-foil folded air cell of a primary surface recuperator is illustrated in Fig. 1. The corrugated pattern maximizes the primary surface area that is in direct contact with exhaust gas on one side and compressor discharge air on the other. Current primary surface recuperators are made of AISI 347 stainless steel foils that operate at gas inlet temperatures of less than 650 °C to attain ~30% efficiency (Omatete, et al., 2000). For low-compression ratios (eg. 5), the efficiency target of greater than 40% is possible with the increase in turbine inlet temperature to 1230 °C, and consequently recuperator inlet temperature to 843 °C. At this elevated temperature levels, the steel foils are susceptible to creep failure due to the fine grain size, accelerated oxidation due to moisture in the hot exhaust gas and loss of ductility due to thermal aging. In addition, severe creep deformation can restrict gas flow, increase recuperator back-pressure and decrease overall efficiency (Rakowski, et al., 2003).

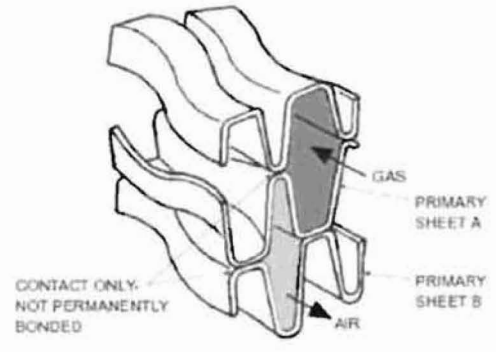

Fig. 1 Schematic of corrugated air-cell in thin foils primary surface recuperator (Aquaro & Pieve, 2007)

The first step in developing recuperators with upgraded performance is to characterize the current technology. Combinations of oxidation and corrosion behavior, and tensile and creep strengths determine the upper temperature and useful lifetime limits. In this respect, creep tests on commercial AISI 347 steel recuperator stock has been conducted. Aging effects on the steel up to 30,000 hours above 700 °C has been established in terms of detrimental sigma phase formation (Minami, et al., 1985). Several stainless alloys including modified 803, alloy 230 and alloy 120 showed better creep strength at 750 °C than AISI 347 stainless steel. In addition, Ni-based superalloys such as alloy 625 and alloy 214 displayed superior creep resistance at this temperature and may be useful at 800 °C or above. Based on these studies, alloy 120 and modified alloy 803 are promising candidates for upgraded recuperator foils (Maziasz & Swinderman, 2003).

An alternate means of improving creep resistance of commercial AISI 347 stainless steel foil is through engineered microstructures. While properties and behavior of AISI 347 steel is generally known for processing and fabrication into other high-temperature components such as heat-exchanger piping and gas turbine parts, information on these alloys fabricated into thin foils (0.1–0.25 mm-thick) for use in primary surface recuperators is limited or nonexistent. Foils with fine grain sizes tend to have less creep resistance relative to coarse-grained products of the same composition. Although Ni-based superalloy such as Inconel 625(Ni-21Cr) has sufficient oxidation and creep resistance for use up to 700 °C, however the cost is 3.5-4 times that of steel (Maziasz, et al., 2004).

The objective of this study is to establish the creep responses and deformation mechanisms of AISI 347 stainless steel foils in temperature ranges typical of advanced recuperators condition. Such data could serve as baseline information for extending the operating temperature limit of AISI 347 austenitic stainless steel foils while maintaining cost competitiveness of the recuperator materials.

2. MATERIALS AND EXPERIMENTAL PROCEDURES

The foil materials used in this study is AISI 347 austenitic stainless steels supplied in the rolled and annealed condition. The foil thickness is 0.25 mm. The chemical composition of the foil is shown in Table 1. The high content of chromium and nickel results in adherent, stable chromium oxide or nickel oxide film for corrosion-resisting property of the material. The addition of (wt. %) 17.8Cr and 11Ni modified the Fe-C phase diagram such that the particularly stable phase austenite that formed at elevated temperature tends to be retained after annealing (Avner, 1974). The low carbon content (0.03%) improves weldability and resistance to carbide precipitation. The addition of Nb further improves in suppressing carbide precipitation at grain boundaries. Fig. 2 shows the microstructure of the as-received foil that consists of austenite matrix with transformed carbide phase. The effect of cold rolling is apparent by the preferred alignment of carbide precipitates along the rolling direction.

Table 1 Chemical composition (wt%) of AISI 347stainless steel foil

Elem	Cr	Ni	Mo	Nb	C
%	17.8	11.0	0.10	0.64	0.03

Si	Mn	Ti	Fe
0.60	1.60	0.04	Bal.

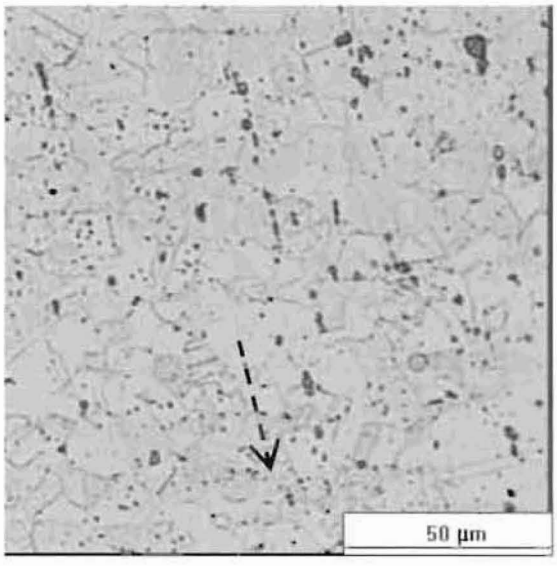

Fig. 2 Microstructure of as-processed AISI 347 stainless steel foil. Rolling direction is indicated by the arrow.

Thin foil creep samples are wire-cut from large sheet to the specimen geometry as illustrated in Fig. 3. A pair of end tabs is design and fabricated from Ti-alloy to mount the foil sample into a standard grip of the creep tester. Continuous creep strains are measured using extensometer equipped with on-line data acquisition system. The knife-edges of the extensometer are mounted between the two rigid end tabs placed at 38 mm apart. Creep-rupture tests are performed at 700±2 °C in a furnace opened to air and with a dead-load machine. Two different applied stress levels used in the creep tests are 238 and 282 MPa.

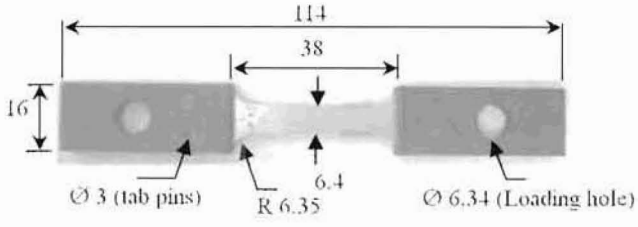

Fig. 3 Thin foil creep specimen fitted with titanium end-tabs and pins. Dimensions in *mm*.

3. RESULTS

Results of the creep-rupture tests are discussed in terms of the measured creep behavior and the observed mechanisms of creep failure.

3.1 Creep Behavior

The resulting creep-rupture behavior of 0.25 mm-thick AISI 347 stainless steel foils at 700 °C is compared in Fig. 4. The creep curve corresponding to the stress of 150 MPa is obtained from literature (Maziasz, et al., 2003). Results show that the primary creep stage is brief and creep life of the foil is dominated by the

secondary and tertiary creep deformation. The time to rupture for AISI 347 foil specimens are 10 and 80 hours for creep tests at constant applied stress of 282 and 238 MPa, respectively. The corresponding creep strain at fracture is 15.4 and 23.8 percent, respectively.

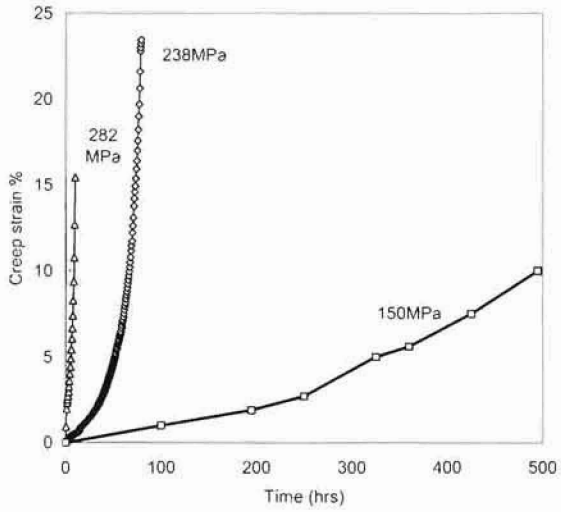

Fig. 4 Comparison of baseline creep curves for AISI 347 stainless steel foil (0.25 mm) in air at 700 °C and different load levels.

In the steady-state creep region, the uniaxial deformation can be expressed in terms of strain rate using the power-law type equation:

$$\dot{\varepsilon}_{ss} = A\sigma^{n}\exp\left(-\frac{Q}{RT}\right) \quad (1)$$

where A and n are creep coefficient and exponent, respectively, Q is the activation energy for creep, the gas constant, $R = 8.314\ J/mol.K$ and T is temperature in Kelvin scale.

The steady-state creep rates for the different applied stress levels for tests at 700 °C are plotted in Fig. 5. The slope of this curve represents the creep exponent, $n = 5.26$ for AISI 347 stainless steel foil material. Utilizing additional limited creep data at 650 and 750 °C (Maziasz, et al., 2004) and assuming identical creep exponent values, the creep coefficient and the corresponding activation energy for creep is determined as $A = 7.947 \times 10^{10}$ and $Q = 556.4\ kJ/mol$. The power-law creep can then be written as:

$$\dot{\varepsilon}_{ss} = 7.947 \times 10^{10}\,\sigma^{5.26}\exp\left(-\frac{66.92 \times 10^{3}}{T}\right) \quad (2)$$

The predicted steady-state creep strain rate extrapolated to lower recuperator working stress level of 50 MPa, 700 °C is $93.68 \times 10^{-12}\ s^{-1}$.

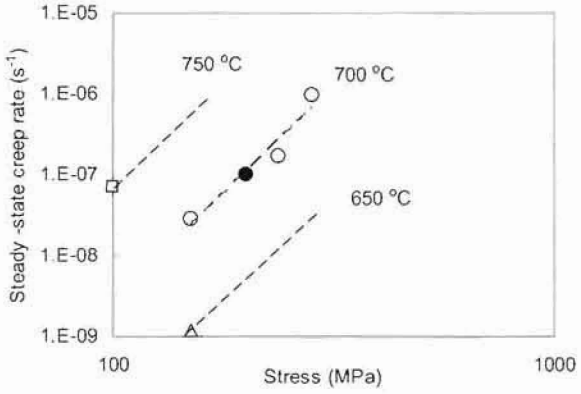

Fig. 5 Steady-state creep rates behavior of AISI 347 stainless steel foils. The dark symbol represents the creep rate for welded foil (Nassour, et al., 2001).

3.2 Creep Failure Mechanisms

Metallographic examination of creep-ruptured foils was performed on sample tested at 700 °C, 282 MPa using optical and scanning electron microscope. Fig. 6 shows the extensive carbides precipitation particularly along the grain boundaries. It is worth noting the larger and elongated grain structure in the vicinity of the fractured plane (right-hand side). This is likely due to the thermally activated anhilation of voids and defects along the grain boundary and the simultaneous stretching of the grains by high localized tensile load. The creep cavitations of *w*-type were seen at the junction of grain boundaries, one is shown in Fig. 7. These voids form at the triple-point grain boundaries where the self diffusion rate is not high enough to relieve the stress concentrations. Under continuous creep straining, these voids can link up to separate the grain boundaries and rapidly weaken the material leading to intergranular fracture.

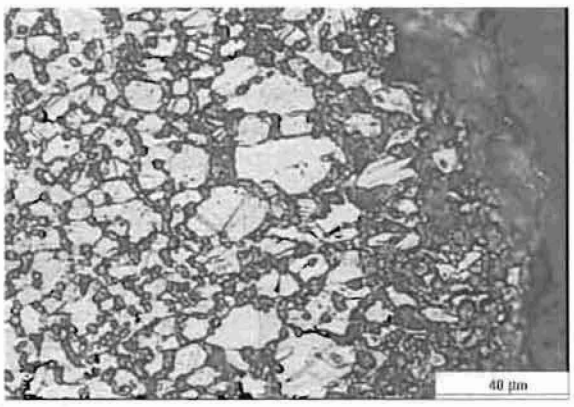

Fig. 6 Microstructure of AISI 347 foil after creep test. Loading direction is horizontal.

At the elevated test temperature of 700 °C, chromium atoms diffuse to the grain boundary and form carbide precipitates. The depletion of adjacent grain matrix in Cr causes sensitization of the alloy leading to loss of the resistance to corrosion. The chromium carbide, $Cr_{23}C_6$ that forms is initially rich in Fe but being replaced by Cr

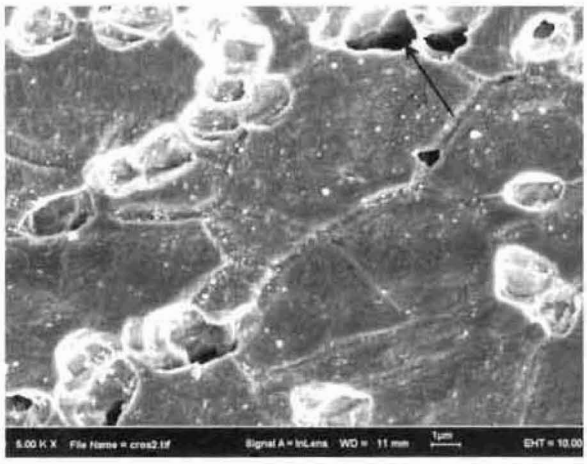

Fig. 7 Creep cavitation at the junction of grain boundaries (indicated by arrow) and growth of carbides along the boundaries.

during the long-time aging under creep condition. Other precipitate found is NbC since the composition is rich in niobium (67.74 wt%), as indicated in Fig. 8.

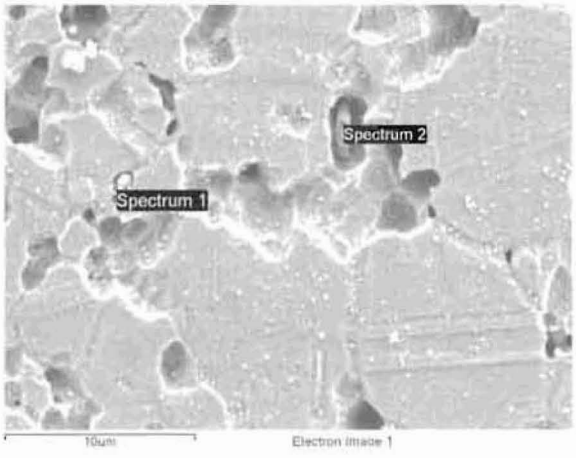

Fig. 8 EDS identification of chromium carbide, $Cr_{23}C_6$ (Spectrum 2) and niobium carbide, NbC (Spectrum 1) in the creep-ruptured foil sample of AISI 347 steel.

CONCLUSIONS

Baseline creep tests on AISI 347 stainless steel foils of thickness 0.25 mm were performed at 700 °C and at different load levels. Results showed that;

- The creep life is dominated by the secondary and tertiary creep stages. The steady-state creep rates follow the power-law creep behavior with creep exponent, $n = 5.26$.
- The activation energy for creep of the rolled and annealed foil is 556.4 kJ/mol
- Extensive precipitation of carbides ($Cr_{23}C_6$ and NbC) are found along the grain boundaries.
- Creep cavitations at triple-point junction of grain boundaries are observed.

ACKNOWLEDGMENT

This study is funded by the Ministry of Science, Technology and Innovation (MOSTI), Malaysia through Science Research Grant No. 79058.

REFERENCES

Aquaro, D. and Pieve, M., Compact Heat Exchangers Optimization Developing a Model for the Thermal-Fluid Dynamic Sizing, *Int. J. of Heat Technology*, vol. 25, pp. 9-18, 2007.

Avner, S. H., *Introduction to Physical Metallurgy*, McGraw-Hill International, New York, USA, 1974.

Maziasz, P. J., Swindeman, R. W., Selecting and Developing Advanced Alloys for Creep-Resistance for Microturbine Recuperator Applications, *J. of Engineering for Gas Turbines and Power*, vol. 125, pp. 310-315, 2003.

Maziasz, P. J., Pint, B. A., Shingledecker, J. P., More, K. L., Evans, N. D., and Lara-Curzio, Austenitic Stainless Steels and Alloys with Improved High-Temperature Performance for Advanced Microturbine Recuperators, *Proc. ASME Turbo Expo 2004*, Vienna, Austria, pp.1-13, 2004.

Maziasz, P. J., Swindeman, R. W., Shingledecker, B. A., More, K. L., Pint, B. A, Lara-Curzio,, E., and Evans, N. D., Improving High-Temperature Performance of Austenitic Stainless Steels for Advanced Microturbine Recuperators, in Parsons 2003: *Engineering Issues in Turbine Machinery, Power Plants and Renewables, The Institute of Materials, Minerals and Mining, Maney*, London, pp. 1057-1073, 2003.

Minami. Y., Kimura, H., and Tanimura, M., Creep rupture properties of 18 pct Cr-8pct Ni-Ti-Nb and type 347H austenitic stainless steels, *J. of Mater Energy Syst*, vol. 7, pp. 45-55, 1985.

Nassour, A., Bose W. W., and Spinelli, D., Creep Properties of Austenitic Stainless-Steel Weld Metals, *J. of Material Engineering and Performance.*, vol. 10, no. 6, pp. 693-698, 2001.

Omatete,O. O., Maziasz, P. J., Pint, B. A., and Stinton, D. P., Assessment of Recuperator Materials for Microturbines, ORNL/TM-2000-304.

Rakowski, J. M., Stinner, C. P., Lipschutz, M., and Montague, J. P., The Use and Performance of Oxidation and Creep-Resistant Stainless in an Exhaust Gas Primary Surface Recuperator Application, *Proc. ASME Turbo Expo 2004*, Vienna, Austria, pp.1-13, 2004.

Hassan OSMAN is current a Ph.D. candidate at the Faculty of Mechanical Engineering, Universiti Teknologi Malaysia.

Mohd Nasir TAMIN completed his Ph.D (1996) in Mechanical Engineering and Applied Mechanics, from University of Rhode Island, USA. He is currently a professor at the Faculty of Mechanical Engineering, Universiti Teknologi Malaysia.